Pore Distribution Changes of Calcium-Based Sorbents Reacting with Sulfur Dioxide

Changes in the pore structure of calcium oxide sorbents derived from calcium carbonate (c-CaO) and calcium hydroxide (h-CaO) reacting with sulfur dioxide are determined. Results show that the pore shape of c-CaO approximates a cylinder while that of h-CaO appears to be slit- or platelike. The pore volume of c-CaO is located in much smaller pores than that of h-CaO when compared on the basis of an equivalent pore shape model. The effect of sintering was to reduce surface area through coalescence of smaller pores, while only minor effects were observed upon pore volume and conversion from calcium oxide to calcium sulfate. Both sorbents expand to allow greater reaction than is possible given the initial porosity and formation of a larger volume product. The h-CaO reacts to higher levels of conversion than the c-CaO because the pore shape of the h-CaO allows for greater particle expansion and, therefore, reaction beyond the limits of the initial porosity.

B. K. Gullett
United States Environmental Protection Agency
Air and Energy Engineering Research Laboratory
Research Triangle Park, NC 27711

K. R. Bruce
Acurex Corporation
Research Triangle Park, 27709

Introduction

The use of limestone-based materials as a medium for adsorbance and chemical reaction with gaseous sulfur dioxide (SO_2) has been extensively studied for reductions of acid rain precursor emissions from utility power plants. Much fundamental research has been conducted to elucidate the physical and chemical mechanisms of this reaction. The reactivity varies with sorbent-specific variables such as chemical form [CaO, $CaCO_3$, $Ca(OH)_2$], source of parent stone, and physical properties (e.g., surface area, porosity). Through a greater understanding of the effect of a sorbent's physical structure upon reactivity, the use of calcium-based sorbent injection may be optimized by sorbent choice and production methods.

Development of extensive internal surface area (Borgwardt and Bruce, 1986) and concurrent pore structure (Hartman and Coughlin, 1974) is necessary for the production of a highly reactive sorbent. Experimental research has shown that a significant amount of internal surface area and pore volume in the reactive form, CaO, resides in the mesopore region (20 to 500 Å) (Beruto et al., 1980). Under optimal conditions, hydrated sorbents have been found to be more reactive than the carbonate form (Cole et al., 1986; Beittel et al., 1985), possibly due to characteristics of their mesopore structure or their smaller particle size resulting from the hydration process. These concepts regarding reactive internal surface area have been used in many investigations to model a sorbent particle's interior physical structure and the mechanistic pathways by which the SO_2 reacts with the CaO (Hartman and Coughlin, 1976; Ramachandran and Smith, 1977; Bhatia and Perlmutter, 1981a; Christman and Edgar, 1983).

In this work research was conducted to examine the pore structure of CaO sorbents derived from calcination of $CaCO_3$ (termed c-CaO), and from $Ca(OH)_2$ (termed h-CaO). The effect of sulfation upon the pore structure at different extents of reaction was examined through sample measurements by nitrogen adsorption/desorption methods. Reactivities were determined by sorbent exposure to SO_2 in an isothermal fixed-bed reactor. The effect of sintering upon the surface area and pore structure, and its influence upon sorbent conversion were examined for both sorbent forms. The structure of the pore system of the sorbents was determined by analysis of the nitrogen adsorption/desorption data with two models for pore structures. The apparent advantage of $Ca(OH)_2$ sorbents was investigated by pore distribution and conversion comparisons of h-CaO with c-CaO.

Experimental Method

The parent sorbent material used in this research was Fredonia White limestone containing 95% $CaCO_3$. The limestone was aerodynamically fractionated using a Donaldson Acucut Particle Classifier to a narrow size distribution with a nominal

Correspondence concerning this paper should be addressed to B. K. Gullett.

value of 2.8 μm. Observation by scanning electron microscopy (SEM) confirmed this particle size. $Ca(OH)_2$ was formed from this parent limestone by first calcining approximately 3 g of $CaCO_3$ to CaO in a N_2-swept (23 std L/min) muffle furnace at 982°C for 90 min. The CaO was then cooled under vacuum and transferred to a filter flask where it was kept under positive N_2 flow. Water (10 mL at 95°C) was added to the flask, and the resulting $Ca(OH)_2$ slurry was dried overnight under flowing N_2. Qualitative observation by SEM showed the resultant median particle diameter to be nominally less than 0.5 μm.

Subsequent calcination of the $CaCO_3$ and dehydration of the $Ca(OH)_2$ were accomplished in an isothermal fixed-bed reactor described by Borgwardt et al. (1984). To obtain c-CaO, a 100 mg sample of the parent $CaCO_3$ was placed evenly on a quartz wool bed and inserted into the reactor at 800°C on a quartz probe. The calcination temperature of 800°C was chosen to minimize surface area loss due to temperature-promoted sintering. Heat-up for 2 min in a stagnant atmosphere was allowed for temperature equilibration prior to beginning 23 std L/min flow of N_2 for an additional 2 min. The N_2 sweep gas removes the CO_2 from $CaCO_3$ during calcination. For preparation of h-CaO, the $Ca(OH)_2$ sample was introduced into the reactor with a preestablished nitrogen flow of 23 std L/min and held there for 60 s. These conditions were chosen because $Ca(OH)_2$ loses water at a lower temperature than $CaCO_3$ loses CO_2 (Beruto et al., 1980), causing the decomposition of the hydroxide to progress to a much greater extent than that of the carbonate during the heat-up time. Also, the presence of water vapor from decomposition of the $Ca(OH)_2$ enhances sintering of h-CaO (Anderson et al., 1965). Both of these factors make it impossible to achieve high surface areas without quickly removing this water at the start of dehydration, thus necessitating the use of a preestablished N_2 flow and shorter times for the production of h-CaO.

Reduced surface areas for both c-CaO and h-CaO were obtained by controlled sintering at 800°C in a stagnant N_2 atmosphere after decomposition to CaO. The production conditions and resultant BET surface area for these sorbents are summarized in Table 1.

The sorbents were reacted immediately following the prescribed calcination/sintering time by quickly switching to an 800°C atmosphere of 7,000 ppm SO_2, 5% O_2, and the balance N_2, for a total process flow of 23 std L/min. The temperature, SO_2 concentration, and total gas throughput were selected in order to approach differential reaction conditions with respect to interparticle SO_2 levels while still allowing an expedient number of samples to be combined for pore size analysis. In addition, a small particle size (<3 μm) was selected to minimize any possible effects caused by diffusion resistance of SO_2 through the intraparticle structure. After SO_2 exposure (times of 5, 25, and 60 s) the sample was removed and cooled under flowing N_2.

Table 1. Production Conditions and BET Surface Area of Sorbents

Series	Material Parent/Product	Time: Heat-up No Flow s	Time: Calcine 23 L/min s	Time: Sinter No Flow s	BET Area m^2/g
A	$CaCO_3$/c-CaO	120	120	0	82.2
B	$CaCO_3$/c-CaO	120	120	5	60.4
C	$CaCO_3$/c-CaO	120	120	10	43.9
D	$Ca(OH)_2$/h-CaO	0	60	0	60.0
E	$Ca(OH)_2$/h-CaO	0	60	5	40.2
F	$Ca(OH)_2$/h-CaO	0	60	10	28.4

Pore size and surface area were determined using a Micromeritics Digisorb 2600 Autoanalyzer. Surface areas were calculated using the BET method and pore distributions were obtained from N_2 adsorption/desorption isotherms. Porosities were determined by measurement of pore volume up to relative pressures of about 0.99, corresponding to pores with nominal openings of 3,000 Å or less. The standard equilibration time between pressure measurements was 5 s. Following these nondestructive analyses, the samples were dissolved in deionized water with 10 mL of 1N HCl, and the extent of reaction, or conversion of CaO by SO_2, calculated from the ratio of $SO_4^=$ ions (determined by ion chromotography) to Ca^{++} ions (determined by atomic absorption spectroscopy). A minimum of three replicates were separately tested to determine reactivity.

The N_2 desorption isotherm was used to derive pore volume data because the desorption value of relative pressure corresponds to the more stable adsorbate condition (Lowell and Shields, 1984). From the Kelvin equation the vapor pressure of a liquid evaporating from a capillary depends on the radius of the capillary, and so the desorption technique will yield data of cumulative volume vs. pore size. Differentiation of this curve produces the pore volume distribution that can be used for purposes of quantitative comparison (an example of this can be seen in Smith, 1981). This was accomplished by adapting an algorithm that used a piecewise-cubic Hermite interpolation, as described in Conte and de Boor (1980).

Initial tests confirmed the reproducibility of the adsorption/desorption isotherms and the experimental technique. Pore structure changes were verified to be caused by sulfation only and not due to sintering caused by the additional reactor exposure time with each sulfation experiment. A sample in flowing N_2 at 800°C retained its pore structure when exposed for an additional 2 min after calcination to simulate the additional reactor residence time of samples exposed to SO_2.

Results and Discussion

Structure

Isotherms for the adsorption and desorption of nitrogen from unreacted c-CaO and h-CaO are shown in Figures 1a and 1b, respectively. Both materials exhibit a type IV isotherm based upon the classification of Brunauer et al. (1940). The type IV isotherm is characteristic of materials with porosity in the mesopore range and that typically exhibit a hysteresis loop (Gregg and Sing, 1982).

The hysteresis loop for the c-CaO is of a shape corresponding to a type A hysteresis [International Union of Pure and Applied Chemistry (IUPAC) designation H1], while the h-CaO shows a type B hysteresis (IUPAC designation H3), according to a revision (Gregg and Sing, 1982) of the de Boer (1958) classification. Type A hysteresis loops are associated with cylindrical pores (Lowell and Shields, 1984) as well as agglomerates of uniform spherical particles (Gregg and Sing), while type B hysteresis is associated with slit-shaped pores or the space between parallel plates (Lowell and Shields).

Further indication of the internal pore structure of these materials can be obtained by use of the *t*-method (Lippens and de Boer, 1965). The isotherm is redrawn as a curve of the volume of N_2 adsorbed, V_a, against the thickness t of the adsorbed

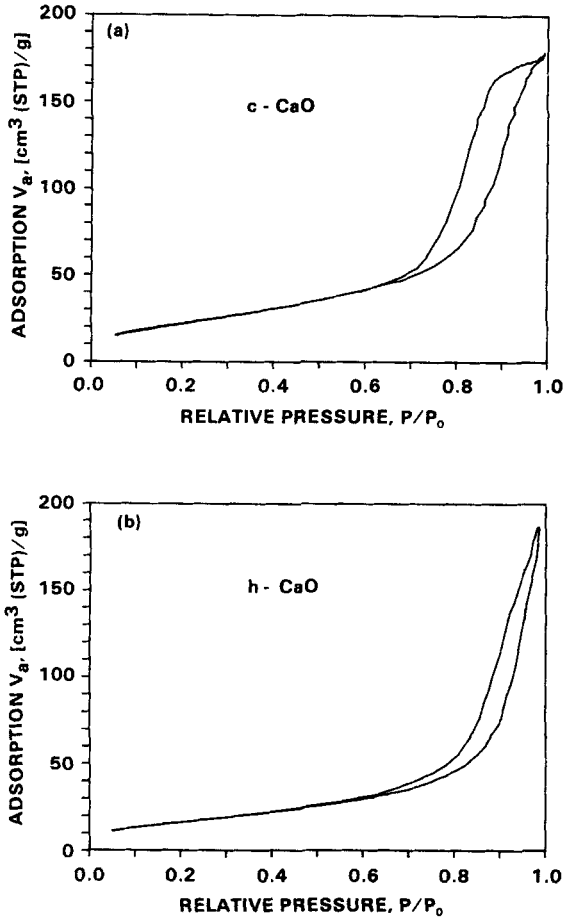

Figure 1. Nitrogen adsorption/desorption isotherms.
a. c-CaO (sample A0)
b. h-CaO (sample F0)

N_2 film at the corresponding relative pressure. This method indicates the deviation of the sample's multilayer formation from that of a freely accessible surface. The thickness equation proposed by de Boer et al. (1966) was used in this work to estimate the value of t from the relative pressure P/P_o. The V_a/t plots, Figure 2, indicate the presence of capillary condensation in both c-CaO and h-CaO by the upward slope that deviates from the initial linear region. This capillary condensation of adsorbate enhances the N_2 uptake at a relative pressure corresponding to a characteristic dimension of the pore determined by the Kelvin equation. For a cylindrical pore geometry, this dimension represents the pore radius, while for a system of parallel plates it represents the pore wall separation d. In this manner, the cylinder pore diameter D is twice the value of d. The eventual leveling-off of the c-CaO curve indicates that many of the pores have filled with adsorbate. For ideal slit-shaped pores, the sides of the slit are parallel, making the radius of curvature infinite; capillary condensation cannot occur at any pressure below saturation. In actual solids, a distribution of wedge-shaped slits allows some condensation to occur (Gregg and Sing, 1982). Further, in a structure that swells or expands, the volume adsorbed in completely filled pore domains would increase with relative pressure according to a capillary condensation mechanism (Broekhoff and van Beek, 1979). Thus, the evidence for apparent capillary condensation with h-CaO indicates deviation from ideal, rigid parallel-wall pores.

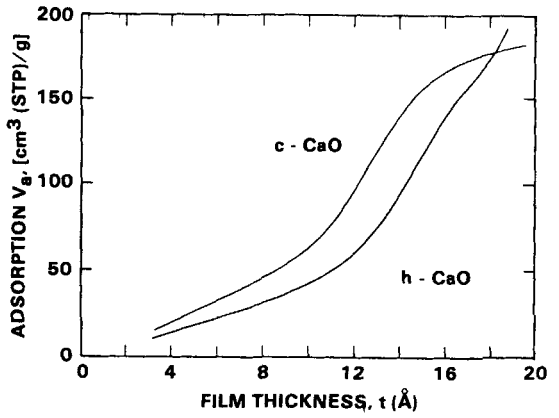

Figure 2. *t*-Method plots, volume of adsorbed nitrogen vs. average thickness of adsorbed film.
Unreacted c-CaO (sample A0), h-CaO (sample F0)
t-values of de Boer et al. (1966) with Harkins and Jura equation (1944)

Further supportive evidence for the deviation of the h-CaO from strictly parallel walls is seen in the isotherm. Closure of a type B hysteresis loop at mid-range pressures is typically characterized by a nearly vertical branch for a narrow distribution of strictly parallel slit widths. With deviations from this ideal case, and with a wide distribution of plate separations, this vertical branch is not seen, and a closure like that of Figure 1b results.

The cylindrical pore structure inferred from the isotherm and hysteresis loops of c-CaO supports similar results of Beruto et al. (1980). Also, the slit or platelike structure found for the h-CaO corroborates their findings for a similarly produced material. A point of major departure from their findings is the shape of the h-CaO V_a/t plot in our work, which indicates apparent capillary condensation in the h-CaO.

The V_a/t plot may also be used as an indicator of the presence or absence of micropores; that is, pores with cylindrical diameter or plate wall separation less than 20 Å (Gregg and Sing, 1982). Extrapolation to a positive intercept on the adsorption axis indicates the presence of micropore volume. Neither h-CaO nor c-CaO shows any evidence of micropore volume, Figure 2. Further, the slope of the V_a/t curve prior to condensation, S_t, is another measure of surface area (Linsen and ven den Heuvel, 1967). The agreement between the BET and S_t values, Table 2, validates the choice of the de Boer thickness equation for this application.

Pore size distributions

The type of physical structure that should be used to model the pore size distribution of the material is determined from

Table 2. Surface Area Comparisons*

	Surface Area, m^2/g	
Sorbent Sample	c-CaO A0	h-CaO D0
BET	82.2	60.0
Model	110.6†	57.3‡
S_t	87.5	65.0

*Calculated from BET theory, pore structure models, and V_a/t plots.
†Cylinder model, ‡Plate model

examination of the isotherms, the hysteresis loops, and the V_a/t plots. For c-CaO, an adaptation (Faass, 1981) of the method of Barrett et al. (1951) is used to model a system of cylindrical pores. This model incorporates the concepts of N_2 adsorbate layer formation and condensation/evaporation at a radius corresponding to the Kelvin equation. The thickness of the adsorbed layer on the pore wall is calculated from the values of de Boer et al. (1966) with the Harkins and Jura (1944) equation. Between pore sizes of 20 and 600 Å, the cylindrical model typically accounted for greater than 95% of the c-CaO pore volume.

The h-CaO materials were modeled by a slit, or parallel-plate pore distribution as developed by Innes (1957). The primary determinant for this choice of model geometry was the type B hysteresis loop (Lowell and Shields, 1984). Between the pore sizes of 20 to 600 Å, the parallel-plate model typically accounted for about 90% of the h-CaO pore volume.

The suitability of a model to reflect pore structure is determined by a comparison of the BET surface area with the surface area predicted by the model from the cumulative increments of pore size. The closer these values, the more confidence that can be placed in the model assumptions (Cranston and Inkley, 1957). As can be seen in Table 2, each model's predicted area is close to that determined by the BET method. Also included are the surface area values S_t determined from the slopes of the V_a/t plots. The results indicate that the cylindrical model does not compare to the BET area of the c-CaO as well as the plate model does for the h-CaO. This may be due to deviations of the pore structure in the c-CaO from the simple, cylindrical model. However, the general agreement of the model results with the BET and S_t values implies that the assumptions for geometrical structure were sufficient to allow for pore structure determinations and comparisons.

Application of the appropriate models to the adsorption/desorption data produces pore structures for the materials that show similar peak volume diameter and plate separation for the c-CaO and h-CaO, respectively. However, if the same physical shape were assumed for the pores of both materials, and the corresponding model used to predict pore volume distributions, the pores of the h-CaO would be larger, the peak volume size approximately doubling that of the c-CaO. This is because the cylindrical pore diameter in the Kelvin equation is equivalent to twice the plate separation (Innes, 1957).

Current modeling efforts of the lime/SO_2 reaction have incorporated assumed physical structures of cylindrical pores (Bhatia and Perlmutter, 1981a, b, Christman and Edgar, 1983), grains (Hartman and Coughlin, 1976), and parallel wedge-shaped pores (Dennis and Hayhurst, 1986).

Effect of sintering

The pore size distributions predicted by the cylindrical model for the c-CaO and the plate model for the h-CaO, are seen in Figure 3. This figure shows three pore distributions each of c-CaO and h-CaO for the unreacted materials of varying surface area. The effect of sintering upon the pore structure of both materials is to significantly reduce the surface area while causing only slight declines in pore volume and, hence, porosity. The pore structure plots in Figure 3 show that the smaller pores disappear, likely coalescing into larger pores, which causes decline of surface area. As an example of this pore size shift, the diameter below which 50% of the c-CaO volume exists changes from

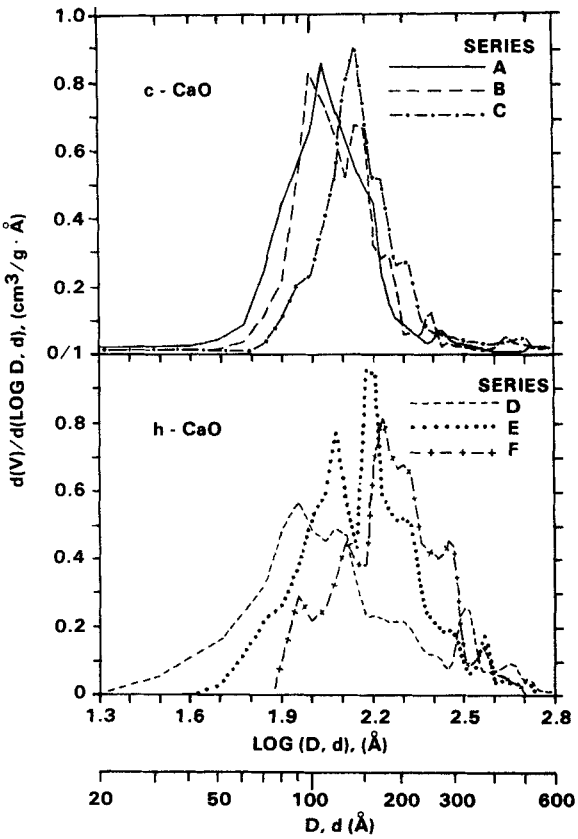

Figure 3. Pore size distributions of unreacted c-CaO and h-CaO.
A, B, C–D, E, F, initial surface areas.
c-CaO, cylindrical pore model; hCaO, plate model

about 110 to 140 Å while the plate separation of h-CaO changes from 105 to 180 Å.

Sintering to lower surface areas at 800°C for up to 10 min had little effect upon sorbent conversion, especially for c-CaO. It is apparent, then, that the smallest pores (under approximately 70 Å dia.), which account for much of the surface area and that are lost during sintering, do not significantly aid the sulfation reaction.

Effect of Reaction

The effect of varying time of SO_2 exposure upon the pore structures of both materials at three initial surface areas can be seen in Figure 4 for c-CaO and Figure 5 for h-CaO. These figures show that the pore volume declines throughout the entire range of pore sizes as the sulfation reaction proceeds. A slight upward shift in the peak pore volume for both c-CaO and h-CaO suggests preferential decline of the pore volume in smaller pores.

The porosity changes of the sorbents during reaction with SO_2 are shown in Figure 6. The c-CaO sorbents lose their pore volume more rapidly and to a greater extent than the h-CaO sorbents as they react.

Conversion

The sorbent conversions up to 240 s exposure to SO_2 are shown in Figure 7. Both materials react quickly, then asymptoti-

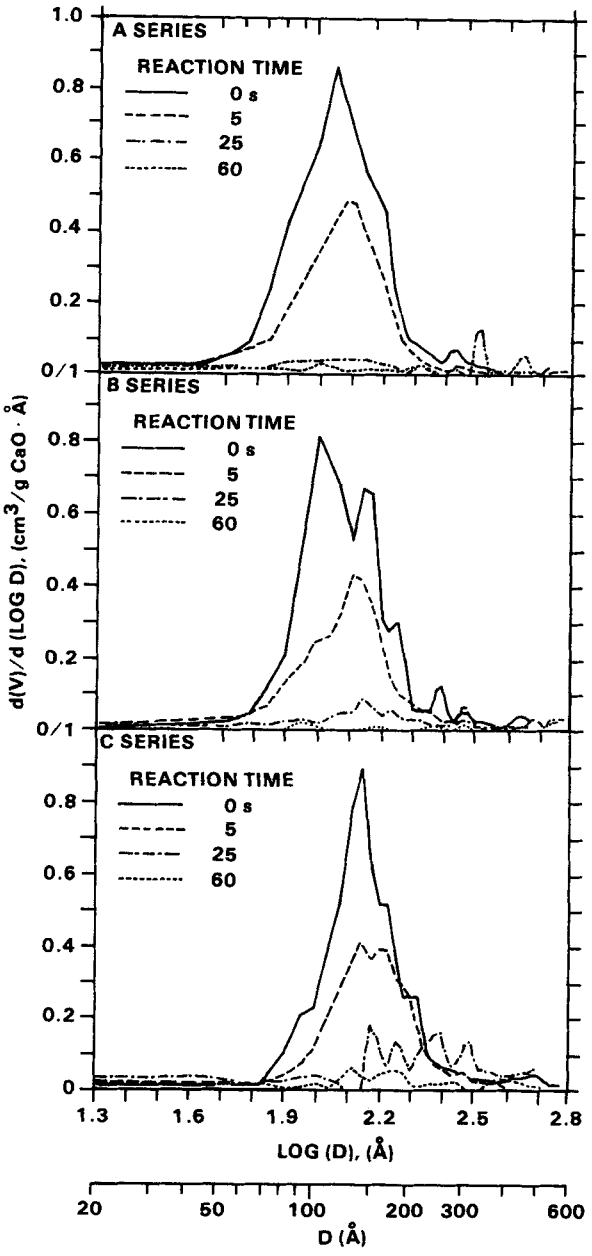

Figure 4. Pore distribution changes in c-CaO at three initial surface areas.

Varying times of exposure to SO_2 at 7,000 ppm, 800°C.

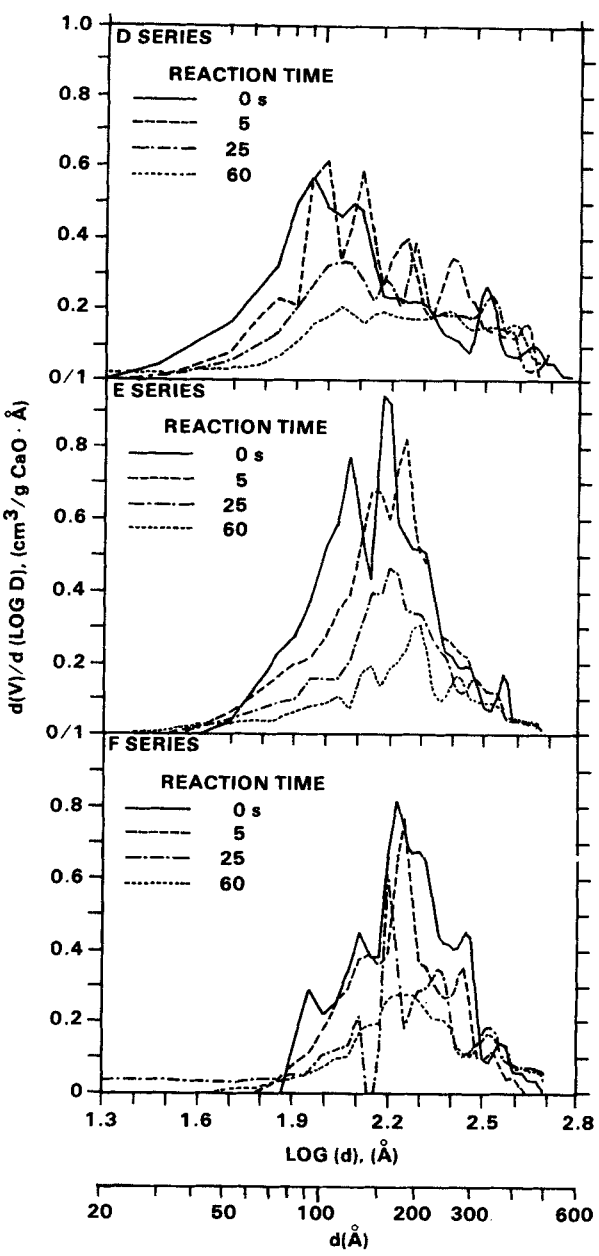

Figure 5. Pore distribution changes in h-CaO at three initial surface areas.

Varying times of exposure to SO_2 at 7,000 ppm, 800°C.

cally approach a peak conversion beyond which little additional reaction occurs. The initial conversion rate of all six materials is similar, reflecting mass transfer control of the reaction. The c-CaO reacts to around 55–60% conversion, while the h-CaO reacts to around 70–80%, although the difference in conversion is only evident at extended times of SO_2 exposure (>40 s). In addition, the effect of initial CaO surface area upon long- or short-term conversion is weak, especially with the C-CaO.

The decline in pore volume and area with reaction is examined in Figure 8 for c-CaO and h-CaO. The pore volume and area appear to decrease in a linear manner with sorbent conversion for both materials. Both values approach zero as conversion is increased. The c-CaO shows a greater rate and percent of area and volume loss than the h-CaO.

The formation of a larger volume product leads to a decline in pore volume through pore filling or pore mouth closure. If the reaction depends upon contact with gaseous SO_2 and intraparticle diffusion resistance is significant, incomplete conversion in the particle interior will result from pore closure at the particle surface. Bhatia and Perlmutter (1981b) noted that surface pore closure will result when the local conversion at the surface equals

$$X_s = \frac{\epsilon_o}{(Z-1)(1-\epsilon_o)}$$

The molar volume ratio, Z, of product to reactant for the sulfation reaction is assumed to be 3.09, adopted in accord with previ-

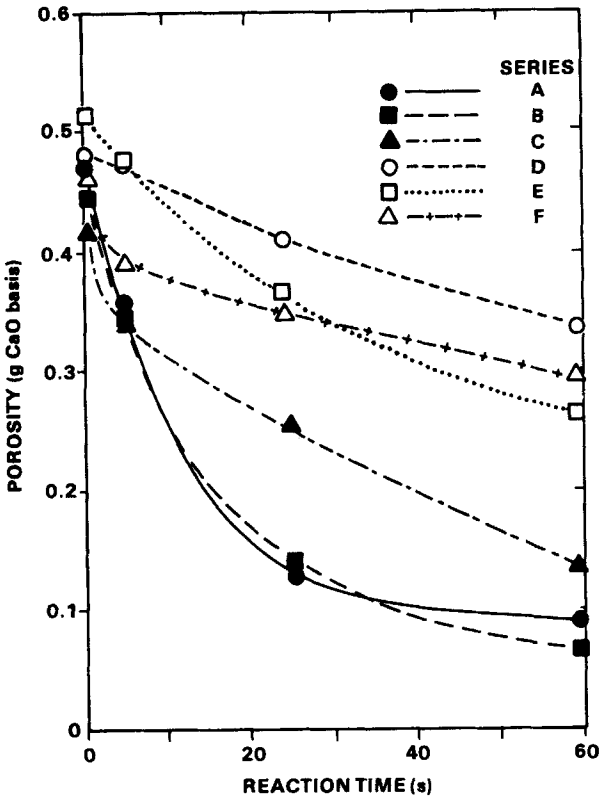

Figure 6. Changes in c-CaO (A, B, C) and h-CaO (D, E, F) porosity.
Reaction with SO_2 at 7,000 ppm, 800°C.

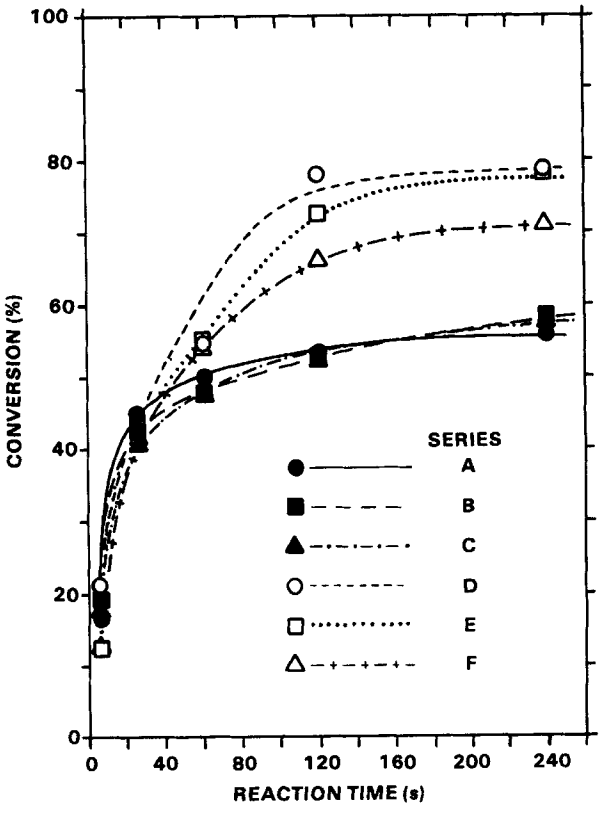

Figure 7. Conversion of c-CaO (A, B, C) and h-CaO (D, E, F).
SO_2 concentration of 7,000 ppm at 800°C.

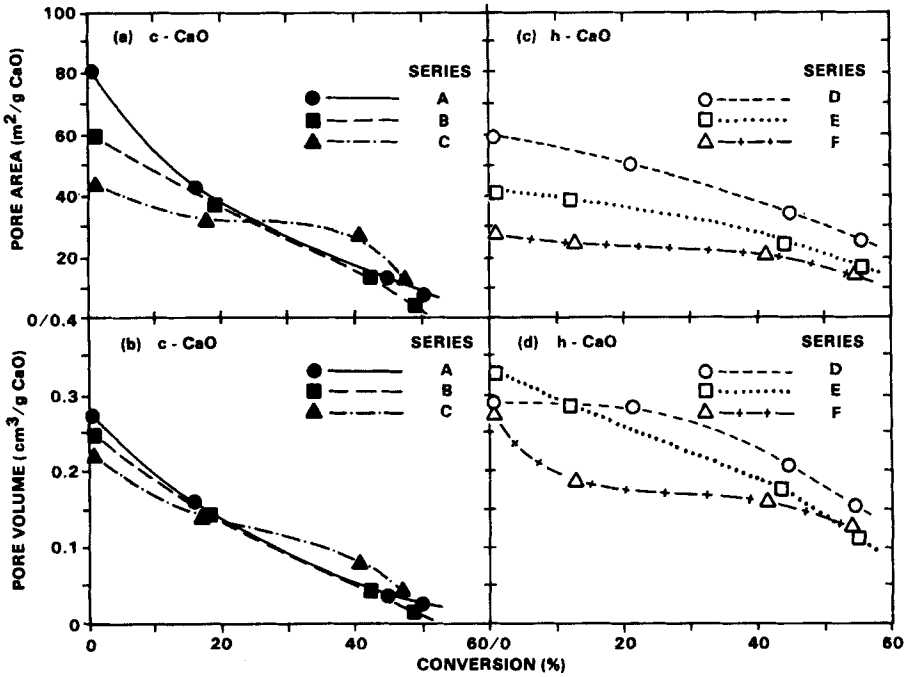

Figure 8. Changes in specific surface area and specific pore volume.
a., b. c-CaO; c., d. h-CaO A, B, C–D, E, F, surface areas reacting with SO_2 at 7,000 ppm, 800°C.

ous work (Hartman et al., 1978; Christman and Edgar, 1983). For this work, X_s equals 0.44 and 0.46 for c-CaO (A0) and h-CaO (D0), respectively. For the very small particle sizes used in this work, pore diffusion is not likely to limit the reaction, and so X_s equals the theoretical limit of sulfation given the initial porosity, a constant particle diameter, and the assumed molar volume ratio. In this case, these X_s values represent about 25 and 35 s of reaction for c-CaO and h-CaO, respectively, Figure 7. For the c-CaO, this time corresponds to the point at which the conversion starts to level off, while the h-CaO still shows considerably more reaction. It is evident that for sulfation to occur beyond the limit imposed by the initial porosity and the greater volume of the product, sulfation of the particle must be accompanied by particle expansion.

This research has shown h-CaO particle expansion by the evidence for a capillary condensation mechanism in the V_a/t plot and the remaining residual porosity beyond the theoretical maximum conversion limit. Additional tests in this research using mercury porosimetry indicate expansion in the interparticle region of h-CaO, supporting findings of particle expansion in sulfated limestone by Borgwardt and Harvey (1972). Further tests with N_2 adsorption/desorption show that changing the pressure equilibration time from 2 to 20 s increases the void space by over 25%, indicating that the nitrogen is capable of expanding the h-CaO. This is supported by other evidence of residual porosity (Hartman and Coughlin, 1976), which may allow continued diffusion of reactants (Bhatia and Perlmutter, 1981a; Pigford and Sliger, 1973) into the particle interior.

The evidence for c-CaO expansion is not as clear. Tests with mercury porosimetry do not indicate significant interparticle expansion, while variation of the equilibration time with the N_2 sorption experiments indicates a 6% increase in void space.

Expansion of both materials during reaction with SO_2 by the amounts apparent from the N_2 adsorption testing would raise X_s to about 0.53 and 0.67 for c-CaO and h-CaO, respectively. These values still fall short of the experimental conversions obtained, indicating that the formation of $CaSO_4$ must produce greater expansion than indicated by N_2 adsorption/desorption techniques.

The faster initial decline of the pore volume and area in the c-CaO for the same amount of conversion supports the conclusion that the pore structure of the c-CaO is more susceptible to reactive closure than the h-CaO. Both materials may have the same intrinsic reactivity, but product formation affects the remaining c-CaO structure differently than the same amount of reaction on the h-CaO. The physical structure of the h-CaO allows for more physical expansion and subsequent retention of porosity than the c-CaO, thereby reducing the effect of a larger volume product upon the decline of porosity.

Conclusions

CaO derived from $CaCO_3$ is composed of a size distribution of cylindrical pores, while CaO derived from $Ca(OH)_2$ forms a pore system of slit or platelike pores. When the isotherm data are evaluated for both CaO derivatives using the same geometrical interpretation of the pore structure, the c-CaO pores are smaller than those of h-CaO.

The pore size distribution of both sorbents shifts to larger pores upon sintering to lower surface areas. Sintering at 800°C for up to 10 min does not have a great effect upon porosity or upon conversion to $CaSO_4$, implying that the surface area lost in the smaller pores does not significantly affect the sorbents' overall conversion.

The effect of reaction with SO_2 is to reduce the pore volume throughout the distribution of pore sizes. The pore volume distribution for both materials shifts to larger pore sizes as reaction occurs, suggesting preferential reaction, sintering, or occlusion of the smaller pores, under approximately 150 Å.

If significant intraparticle diffusion resistance exists, then a product layer would form, resulting in surface pore closure and incomplete conversion in the center of the particle. However, in this work both materials react beyond the conversion levels expected by complete loss of initial porosity to the greater volume of the product, $CaSO_4$. This implies that intraparticle diffusion resistance is not significant and that expansion of the particle is necessary to account for these conversion levels.

For conversion levels beyond 45%, the h-CaO reacts to a higher value than the c-CaO under these experimental conditions. This is due to greater retention of porosity by h-CaO than c-CaO at similar levels of conversion. The platelike structure of the h-CaO allows for greater particle expansion, maintaining higher porosity.

Acknowledgment

This work was supported by the U.S. Environmental Protection Agency's Air and Energy Engineering Research Laboratory. The authors are grateful to Cathleen O'Neil of Micromeritics Instrument Corporation for her assistance with nitrogen porosimetry.

Notation

d = plate separation
D = pore diameter
P = vapor pressure of adsorptive gas
P_o = saturation vapor pressure of adsorptive gas
S_t = surface area from t-method
t = average film thickness
T = temperature
V = volume of liquid nitrogen adsorbed
V_a = volume of gaseous nitrogen adsorbed
X_s = local conversion of CaO to $CaSO_4$, atom S per atom Ca
Z = molar volume ratio of $CaSO_4$ to CaO
ϵ_o = initial porosity

Literature Cited

Anderson, P. J., R. F. Horlock, and R. G. Avery, "Some Effects of Water Vapour during the Preparation and Calcination of Oxide Powders," *Proc. Brit. Ceram. Soc.*, **3**, 33 (1965).

Barrett, E. P., L. G. Joyner, and P. P. Halenda, "The Determination of Pore Volume and Area Distributions in Porous Substances. I: Computations from Nitrogen Isotherms," *J. Am. Chem. Soc.*, **73**, 373 (1951).

Beittel, R., J. P. Gooch, E. B. Dismukes, and L. J. Muzio, "Studies of Sorbent Calcination and SO_2-Sorbent Reactions in a Pilot-scale Furnace," *Proc. 1st Joint Symp. on Dry SO_2 and Simul. SO_2/NO_x Control Technol.* **1**, EPA-600/9-85-020a (NTIS PB85-232353), p. 16-1 (July, 1985).

Beruto, D., L. Barco, A. W. Searcy, and G. Spinolo, "Characterization of the Porous CaO Particles Formed by Decomposition of $CaCO_3$ and $Ca(OH)_2$ in Vacuum," *J. Am. Cer. Soc.*, **63**, 439 (1980).

Bhatia, S. K., and D. D. Perlmutter, "The Effect of Pore Structure on Fluid-Solid Reactions: Application to the SO_2-Lime Reaction," *AIChE J.*, **27**, 226 (1981a).

———, "A Random-Pore Model for Fluid-Solid Reactions. II: Diffusion and Transport Effects," *AIChE J.*, **27**, 247 (1981b).

Borgwardt, R. H., and K. R. Bruce, "Effect of Specific Surface Area on the Reactivity of CaO with SO_2," *AIChE J.*, **32**, 239 (1986).

Borgwardt, R. H., and R. D. Harvey, "Properties of Carbonate Rocks Related to SO_2 Reactivity," *Environ. Sci. Technol.*, **6**, 350 (1972).

Borgwardt, R. H., N. F. Roache, and K. R. Bruce, "Surface Area of Calcium Oxide and Kinetics of Calcium Sulfide Formation," *Environ. Prog.*, **3**, 129 (1984).

Broekhoff, J. C. P., and W. P. van Beek, "Scanning Studies on Capillary Condensation and Evaporation of Nitrogen," *J. Chem. Soc., Faraday Trans. I*, **75**, 42 (1979).

Brunauer, S., L. Deming, W. Deming, and E. Teller, "On a Theory of the van der Waals Adsorption of Gases," *J. Am. Chem. Soc.*, **62**, 1723 (1940).

Christman, P. G., and T. F. Edgar, "Distributed Pore-Size Model for Sulfation of Limestone," *AIChE. J.*, **29**, 388 (1983).

Cole, J. A., J. C. Kramlich, W. R. Seeker, G. D. Silcox, G. H. Newton, D. J. Harrison, and D. W. Pershing, "Fundamental Studies of Sorbent Reactivity in Isothermal Reactors," 2nd Joint Symp. on Dry SO_2 and Simul. SO_2/NO_x Control Technol. EPA/EPRI, Raleigh, NC (June, 1986).

Conte, S., and C. de Boor, *Elementary Numerical Analysis: An Algorithmic Approach*, 3rd ed., McGraw-Hill, New York, 286 (1980).

Cranston, R. W., and F. A. Inkley, "The Determination of Pore Structures from Nitrogen Adsorption Isotherms," *Adv. Catal.*, **9**, 143 (1957).

de Boer, J. H., *The Structure and Properties of Porous Materials, Tenth Colston Symposium*, D. H. Everett, F. S. Stone, eds., Butterworths, London, 68 (1958).

de Boer, J. H., B. C. Lippens, B. G. Linsen, J. C. P. Broekhoff, A. van den Heuvel, and T. J. Osinga, "The *t*-Curve of Multimolecular N_2-Adsorption," *J. Colloid Interf. Sci.*, **21**, 405 (1966).

Dennis, J. S., and A. N. Hayhurst, "A Simplified Analytical Model for the Rate of Reaction of SO_2 with Limestone Particles," *Chem. Eng. Sci.*, **41**, 25 (1986).

Faass, G. S., "Correlation of Gas Adsorption, Mercury Intrusion, and Electron Microscopy Pore Property Data for Porous Glasses," M. Sc. Thesis, Georgia Inst. Technol., Atlanta (1981).

Gregg, S. J., and K. S. W. Sing, *Adsorption, Surface Area, and Porosity*, 2nd ed., Academic Press, London (1982).

Harkins, W. D., and G. Jura, "Surfaces of Solids. XIII: A Vapor Adsorption Method for the Determination of the Area of a Solid without the Assumption of a Molecular Area, and the Areas Occupied by Nitrogen, and Other Molecules on the Surface of a Solid," *J. Am. Chem. Soc.*, **66**, 1366 (1944).

Hartman, M., and R. W. Coughlin, "Reaction of Sulfur Dioxide with Limestone and the Influence of Pore Structure," *Ind. Eng. Chem. Process Des. Dev.*, **13**, 248 (1974).

———, "Reaction of Sulfur Dioxide with Limestone and the Grain Model," *AIChE J.*, **22**, 490 (1976).

Hartman, M., J. Pata, and R. W. Coughlin, "Influence of Porosity of Calcium Carbonates on Their Reactivity with Sulfur Dioxide," *Ind. Eng. Chem. Process Des. Dev.*, **17**, 411 (1978).

Innes, W. B., "Use of a Parallel Plate Model in Calculation of Pore Size Distribution," *Anal. Chem.*, **29**, 1069 (1957).

Lippens, B. C., and J. H. de Boer, "Studies on Pore Systems in Catalysts. V: The *t*-method," *J. Catal.* **4**, 319 (1965).

Linsen, B. G., and A. van den Heuvel, "Pore Structures," *The Solid-Gas Interface*, **2**, E. A. Flood, ed., Dekker, New York, 1025 (1967).

Lowell S., and J. E. Shields, *Powder Surface Area and Porosity*, 2nd ed., Chapman and Hall, London (1984).

Pigford, R. L., and G. Sliger, "Rate of Diffusion-Controlled Reaction Between a Gas and a Porous Solid Sphere," *Ind. Eng. Chem. Process Des. Dev.*, **12**, 85 (1973).

Ramachandran, P. A., and J. M. Smith, "A Single-Pore Model for Gas-Solid Noncatalytic Reactions," *AIChE J.*, **23**, 353 (1977).

Smith, J. M., *Chemical Engineering Kinetics*, 3rd. ed., McGraw-Hill, New York (1981).

Manuscript received Oct. 2, 1986, and revision received Mar. 31, 1987.